Nonadiabatic tunnel ionization of current-carrying orbitals of prealigned linear molecules in strong circularly polarized laser fields

Kunlong Liu and Ingo Barth*
Max Planck Institute of Microstructure Physics, Weinberg 2, D-06120 Halle (Saale), Germany
(Received 12 August 2016; published 3 October 2016)

We derive the analytical formula of the ratio of the ionization rates of degenerate valence $\pi_\pm$ orbitals of prealigned linear molecules in strong circularly polarized (CP) laser fields. Interestingly, our theory shows that the ionization ratio for molecular orbitals with opposite azimuthal quantum numbers $\pm|m|$ (e.g., $\pi_\pm$) is identical to that for atomic orbitals with the same $\pm|m|$ (e.g., $p_\pm$). In general, the electron counter-rotating to the CP laser field tunnels more easily, not only for atoms but also for linear molecules. Our theoretical predictions are then verified by numerically solving the three-dimensional time-dependent Schrödinger equation for the ionization of the prealigned nitric oxide (NO) molecule in strong CP laser fields. Due to the spin-orbital coupling in the electronic ground state of NO and the sensitivity of ionization to the sense of electron rotation, the ionization of NO in CP fields can produce spin-polarized photoelectrons with high controllability of spin polarization up to 100%.

DOI: 10.1103/PhysRevA.94.043402

I. INTRODUCTION

In the late 1960s, the theory of nonadiabatic tunnel ionization of atoms in strong laser fields was developed. In this theory for short-range potentials, known as PPT theory, the analytical expressions of the ionization rates were derived for all atomic valence orbitals in linearly polarized laser fields as well as for nondegenerate s valence orbitals in circularly or elliptically polarized laser fields [1–3]. A few years ago, the theory has been extended to obtain analytical expressions of the ionization rates for degenerate valence $p_\pm$ and p_0 orbitals in strong circularly polarized (CP) laser fields [4,5]. This theoretical result provides better understanding of the ionization of valence atomic p orbitals of noble gas in strong CP laser fields. While the ionization of p_0 orbitals is suppressed very well due to the destructive interference from two phase-opposite lobes, the theory predicts that the electron counter-rotating to the CP laser field tunnels easier than the co-rotating electron. For example, for right CP laser fields, the ionization of the current-carrying p_- orbital is preferred over the oppositely current-carrying p_+ orbital. This prediction has been partially confirmed by the sequential double ionization experiment [6,7] and verified by numerical calculations by solving the two-dimensional (2D) time-dependent Schrödinger equation (TDSE) [8]. However, for very strong and low-frequency laser fields, the ionization preference can be changed. This effect has been explained by using the three-level model of Floquet theory, where the adiabatic laser-dressed orbitals play an important role [8]. It has also been shown that nonrelativistic strong-field tunnel ionization of the valence p shell can produce spin-polarized photoelectrons [9]. It is due to the spin-orbit couplings in the ionic states $P_{3/2}$ and $P_{1/2}$ of noble gas and the sensitivity of ionization to the sense of initial electron rotation. However, due to fourfold degeneracy of the ionic ground state $P_{3/2}$, spin polarization of photoelectrons can reach only up to 50%.

In this work, we develop the theory of tunnel ionization of prealigned linear molecules possessing degenerate orbitals in strong CP laser fields. Electronic ring currents in excited degenerate $\pi_\pm$ orbitals of prealigned linear molecules can be prepared by weak CP laser pulses; see Refs. [10,11]. Here, we investigate ionization of current-carrying valence $\pi_\pm$ orbitals of nitric oxide (NO). Since NO has only one electron in the valence π shell, the electronic ground state $|\Pi_\pm\rangle$ is doubly degenerate. Based on our experience that the counter-rotating electron in atoms tunnels more easily, we expect that this interpretation is also valid for degenerate molecular orbitals, i.e., the ionization of the prealigned π_- orbital is in general preferred over π_+ in strong right CP laser fields. With some thoughts about conservation of the z component of the electronic angular momentum, we derive the ratio of the ionization rates of valence $\pi_\pm$ orbitals. Furthermore, we derive the improved formula of the ionization ratio for very strong and low-frequency laser fields, by setting the Floquet wave function as the initial wave function in the derivation of the formulas of the ionization rates. To test the validity of our theory, we perform three-dimensional (3D) TDSE for the tunnel ionization of the prealigned NO in strong three-cycle CP laser pulses.

In contrast to noble gas atoms where the ground state is nondegenerate and the ionic state is degenerate, the electronic ground state of NO is degenerate and has spin-orbit coupling. It splits into two doubly degenerate states $|\Pi_{1/2}\rangle$ and $|\Pi_{3/2}\rangle$ with energy splitting of about $120\,\mathrm{cm}^{-1}$. The ground state $|\Pi_{1/2}\rangle$ has two possible electron configurations $\pi_+^\downarrow$ and $\pi_-^\uparrow$. Because we expect that ionization rates for π_+ and π_- molecular orbitals are different, we predict that nonadiabatic strong-field tunnel ionization of NO can produce photoelectrons with spin polarization up to 100% thanks to the lower degeneracy of molecular orbitals compared to that of atomic $p_{3/2}$ orbitals.

This paper is organized as follows. In Sec. II, we derive the analytical formula of the ratio of the ionization rates of valence $\pi_\pm$ orbitals of prealigned molecules in strong CP laser fields. In addition, we derive the improved formula for very strong and low-frequency laser fields, using the three-level

*barth@mpi-halle.mpg.de

model of Floquet theory. In Sec. III, we perform 3D TDSE for ionization of NO in strong CP laser pulses with different laser amplitudes and laser wavelengths. In Sec. IV, we discuss the results of our theoretical and numerical calculations and show that highly spin-polarized photoelectrons can be produced. Section V concludes this work.

II. THEORY

As already shown in the theory of nonadiabatic tunnel ionization of atoms for short-range potentials in strong continuous wave (cw) laser fields (PPT theory) [1–3], the form of the wave function in the asymptotic region is essential for calculation of the ionization rate of the atomic valence orbital. For short-range potentials, the wave function in spherical coordinate representation $\mathbf{r} = (r,\theta_r,\phi_r)$ asymptotically far from the atomic core is [1,5]

$$\varphi_{lm}(\mathbf{r} \to \infty) = C_{\kappa l}\kappa^{3/2}\frac{e^{-\kappa r}}{\kappa r}Y_{lm}(\theta_r,\phi_r), \tag{1}$$

with the constant $C_{\kappa l}$, depending on $\kappa = \sqrt{2I_p}$ or ionization potential I_p and total angular momentum quantum number l as well as details of the potential near the atomic core. For atoms, the azimuthal or magnetic quantum number m is also a good quantum number, therefore asymptotic wave functions of valence atomic orbitals are characterized by quantum numbers $l \in \mathbb{N}_0$ and $m = -l,-l+1,\ldots,l-1,l$.

Since linear molecules prealigned along the z axis (here propagation axis of the CP laser field) have no spherical symmetry, the quantum number l is no longer a good quantum number, whereas the magnetic quantum number m is still a good quantum number, because the z component of the angular momentum operator commutes with field-free Hamiltonian for linear molecules. Thus, the wave functions of valence orbitals of prealigned linear molecules are then characterized only by the quantum number $m \in \mathbb{Z}$. As suggested by Tong *et al.* [12], see also Ref. [13], and in case of short-range potentials, the asymptotic wave function with given magnetic quantum number m for linear molecules can be expressed as linear combination of Eq. (1),

$$\varphi_m(\mathbf{r} \to \infty) = \frac{1}{\sqrt{\kappa}}\sum_{l=|m|}^{\infty}\varphi_{lm}(\mathbf{r} \to \infty) \tag{2}$$

$$= \frac{e^{-\kappa r}}{r}\sum_{l=|m|}^{\infty}C_{\kappa l}Y_{lm}(\theta_r,\phi_r), \tag{3}$$

where the sum is over l ranging from $|m|$ to infinity. The real coefficients $C_{\kappa l}$ for valence orbitals of linear molecules are fitted such that the asymptotic wave function is similar to the exact wave function of linear molecules in the asymptotic regime. These coefficients for some linear molecules beyond short-range potentials are listed in Refs. [12,13].

Using spherical harmonics,

$$Y_{lm}(\theta_r,\phi_r) = \sqrt{\frac{2l+1}{4\pi}\frac{(l-m)!}{(l+m)!}}P_l^m(\cos\theta_r)e^{im\phi_r}, \tag{4}$$

and the relation for associated Legendre polynomials,

$$P_l^{-m}(\cos\theta) = (-1)^m\frac{(l-m)!}{(l+m)!}P_l^m(\cos\theta), \tag{5}$$

we obtain from Eq. (3) for $m = |m|$

$$\varphi_{|m|}(\mathbf{r} \to \infty) = \frac{e^{-\kappa r}}{r}e^{im\phi_r},$$
$$\sum_{l=|m|}^{\infty}C_{\kappa l}\sqrt{\frac{2l+1}{4\pi}\frac{(l-|m|)!}{(l+|m|)!}}P_l^{|m|}(\cos\theta_r), \tag{6}$$

and for $m = -|m|$,

$$\varphi_{-|m|}(\mathbf{r} \to \infty) = \frac{e^{-\kappa r}}{r}e^{-i|m|\phi_r}(-1)^{|m|},$$
$$\sum_{l=|m|}^{\infty}C_{\kappa l}\sqrt{\frac{2l+1}{4\pi}\frac{(l-|m|)!}{(l+|m|)!}}P_l^{|m|}(\cos\theta). \tag{7}$$

The additional factor $(-1)^{|m|}$ for negative m is not important, since it changes only the sign of the whole wave function for odd m and it does not affect the ionization rate. In particular, the probability of the n-photon process (see Ref. [5]), depends on the magnitude of the wave function in momentum representation and the factor $(-1)^{|m|}$ then vanishes.

The only one difference between asymptotic wave functions for positive and negative m is the exponent $e^{im\phi_r}$, that is already factored out in Eqs. (6) and (7), whereas the sum of terms over l does not depend on the sign of m. We note that in the spherical momentum representation $\mathbf{v} = (v,\theta_v,\phi_v)$, the probability of the n-photon process depends on $|e^{im\phi_{v\pm}(t_i)}|^2$, where $\mathbf{v}_\pm(t_i)$ is the initial electron velocity at the complex ionization time t_i for the right (+) or left (−) CP laser field [5]. Because t_i and thus $\phi_{v\pm}(t_i)$ are complex, the magnitude of this exponent is not equal to 1. Therefore, the ionization rate is different for positive and negative m for given circular polarization. It has been predicted and verified by numerical calculations for degenerate atomic orbitals in strong CP laser fields [4,5,8], that the tunnel ionization of the counter-rotating orbital with respect to the circular polarization of the laser field is preferred. For example, the p_- electron tunnels more easier than the p_+ electron in the strong right CP laser field.

Of course, the ionization rates for atomic and molecular orbitals are different because the atomic wave function has only one l component [Eq. (1)] whereas the wave function of the linear molecule has many l components [Eq. (3)]. However, since the wave functions for positive and negative m in Eqs. (6) and (7) except for the exponent $e^{im\phi_r}$ are identical not only for atoms (with only one l component) but also for linear molecules, we predict that the ratio of the ionization rates of degenerate orbitals with opposite $\pm|m|$ are identical for atoms and linear molecules. It can be verified by straightforward derivation of the ionization rates of degenerate orbitals by using the general asymptotic wave function for short-range potentials [Eq. (3)] in exactly the same way as the derivation in Ref. [5]. The analytical expression of the ratio of the ionization

rates of degenerate orbitals with $m = \pm 1$ is [4,5,8]

$$R_{\pm} = \frac{w_{\pm}^{-}}{w_{\pm}^{+}} = \left(\frac{\sqrt{\zeta_0^2 + \gamma^2} \pm \zeta_0 \sqrt{1+\gamma^2}}{\sqrt{\zeta_0^2 + \gamma^2} \mp \zeta_0 \sqrt{1+\gamma^2}} \right)^2, \tag{8}$$

where $w_{\pm}^{m}$ is the ionization rate for right (+) or left (−) circular polarization and for positive ($m = +1$) or negative ($m = -1$) magnetic quantum number. In Eq. (8), γ is the Keldysh parameter,

$$\gamma = \frac{\omega}{\mathcal{E}} \sqrt{2 I_p}, \tag{9}$$

with the electric field amplitude $\mathcal{E}$ and laser frequency ω of the cw CP laser field and $\zeta_0(\gamma) > 0$ is the solution of the transcendental equation,

$$\operatorname{arctanh} \sqrt{\frac{\zeta_0^2 + \gamma^2}{1+\gamma^2}} = \frac{1}{1-\zeta_0} \sqrt{\frac{\zeta_0^2 + \gamma^2}{1+\gamma^2}}. \tag{10}$$

We emphasize that the result [Eq. (8)] is not only for atoms but also for linear molecules, where $m = \pm 1$ is the magnetic quantum number for atoms or linear molecules, in general for systems having at least cylindrical symmetry. In particular, the ionization ratio $R_{\pm}$ depending on circular polarization ($\pm$) for linear molecules is the same as for atoms. Thus, the analytical expression of the ratio of the ionization rates of π_- and π_+ molecular orbitals ($m = \pm 1$) and the ratio of the ionization rates of p_- and p_+ atomic orbitals ($m = \pm 1$) is identical for short-range potentials and cw CP laser fields. This interpretation can be generalized for other orbitals with $|m| > 1$, for example, the ionization ratios for δ_- and δ_+ molecular orbitals and for d_- and d_+ atomic orbitals are identical, and so on. We note that in this derivation as in the PPT theory the ratio of ionization rates of orbitals with opposite $\pm|m|$ do not change if adiabatic effects of the long-range Coulomb potential are included [3,14,15]. However, we neglect nonadiabatic Coulomb effects, which can be ignored for small γ; for more details see Ref. [15].

Finally, for very strong laser fields and low laser frequencies (small γ), degenerate atomic and molecular orbitals modify adiabatically prior to tunnel ionization. As already shown by numerical calculation for atomic orbitals and explained by the three-level model of Floquet theory [8], the preference of tunnel ionization is changed in the regime of small γ, i.e., the co-rotating electron tunnels easier than the counter-rotating electron. In particular, for strong and low-frequency right CP laser fields, the field-free atomic p_+ and p_- orbitals modify adiabatically to laser-dressed $p_{\parallel}$ and $p_{\perp}$ orbitals, where $p_{\parallel}$ and $p_{\perp}$ orbitals are aligned along and perpendicular to the rotating electric field vector, respectively. Since the ionization of the $p_{\parallel}$ orbital is preferred over $p_{\perp}$, the ionization of the atomic p_+ orbital is thus preferred in the regime of small γ. We figure out that the theoretical results for laser-dressed atomic orbitals can be used for laser-dressed orbitals of linear molecules, since only the value of the magnetic quantum number m (same for atoms and linear molecules) is essential for ionization in strong CP laser fields.

As suggested in Ref. [8], the periodic Floquet wave function $\varphi_{\pm,m}^{F}(\mathbf{r},t)$ for given circular polarization ($\pm$) and magnetic quantum number $m = \pm 1$ can be expressed as superposition of field-free nondegenerate (first excited) $\varphi_0(\mathbf{r})$ and degenerate valence $\varphi_m(\mathbf{r})$ orbitals as

$$\varphi_{\pm,m}^{F}(\mathbf{r}) = b_{\pm,m}^{0} \varphi_0(\mathbf{r}) + b_{\pm,m}^{+} \varphi_+(\mathbf{r}) e^{\mp i\omega t} + b_{\pm,m}^{-} \varphi_-(\mathbf{r}) e^{\pm i\omega t}. \tag{11}$$

To calculate the numerical values of quasienergies $E_{\pm,m}^{F}$ and real coefficients $b_{\pm,m}^{0}, b_{\pm,m}^{+}$, and $b_{\pm,m}^{-}$, we need values of field-free eigenenergies E_0, E_m of these three orbitals, dipole matrix element $\mathbf{D} = \langle \varphi_0 | \mathbf{r} | \varphi_+ \rangle = D(\mathbf{e}_x + i\,\mathbf{e}_y)$, laser amplitude $\mathcal{E}$, and laser frequency ω. The corresponding formulas are given in Ref. [8]. We note that the coefficient $b_{\pm,m}^{0}$ is negligible, i.e., the distortion of the wave function is small, whereas the alignment of the wave function determined by large coefficients $b_{\pm,m}^{\pm}$ plays an important role [8]. We can neglect $b_{\pm,m}^{0}$ for the derivation of the ionization rate, but the dipole moment D from φ_0 and φ_+ is necessary because it determines $b_{\pm,m}^{\pm}$.

Using the Floquet wave function [Eq. (11)] in the asymptotic regime $\varphi_{\pm,m}^{F}(\mathbf{r} \to \infty)$ as the initial wave function for $m = \pm 1$ prior to tunnel ionization, we derive the ionization rates for laser-dressed valence orbitals of atoms or linear molecules. The derivation of the ionization rates is straightforward as in Ref. [5] and we here omitted the long derivation. The final result for the ratio of the ionization rates of adiabatically modified orbitals with $m = \pm 1$ is

$$R_{\pm}^{F} = \frac{w_{\pm}^{F,-}}{w_{\pm}^{F,+}} = \left(\frac{b_{\pm,-}^{+} + b_{\pm,-}^{-} \sqrt{R_{\pm}}}{b_{\pm,+}^{+} + b_{\pm,+}^{-} \sqrt{R_{\pm}}} \right)^2, \tag{12}$$

where $w_{\pm}^{F,m}$ is the corresponding ionization rate including the three-level model of Floquet theory. For large Keldysh parameters γ, the modified ratio $R_{\pm}^{F}$ becomes $R_{\pm}$, because $b_{\pm,-}^{+} \to 0$, $b_{\pm,-}^{-} \to 1$, $b_{\pm,+}^{+} \to 1$, and $b_{\pm,+}^{-} \to 0$; see Ref. [8].

III. NUMERICAL CALCULATION

In order to verify the prediction of our theory, we choose the NO molecule and perform *ab initio* calculations of the ionization of NO in strong CP laser pulses. The linear molecule NO is a suitable candidate for our study because the highest occupied molecular orbitals (HOMO) are degenerate $\pi_{\pm}$ orbitals and the ground state $|X\,^2\Pi_{\pm}\rangle$ is doubly degenerate.

To date, the exact numerical solution of the 3D TDSE for a molecule with multiple electrons in strong laser fields is unfeasible. But, since the valence shell of the NO molecule consists of only one electron, it is reliable to apply the single active electron (SAE) approximation to the interaction of the NO molecule with the laser field. In numerical calculations, the molecule is prealigned along the z axis of the Cartesian coordinate system and the CP laser field is propagated along the molecular axis (see Fig. 1). The length-gauge 3D TDSE for the single-electron wave function, $\Psi(\mathbf{r},t) = \Psi(x,y,z,t)$, in the dipole approximation is given by (atomic units are used unless stated otherwise)

$$i \frac{\partial}{\partial t} \Psi(\mathbf{r},t) = \left[-\frac{\nabla^2}{2} + V_{\text{eff}}(\mathbf{r}) + \mathbf{r} \cdot \mathbf{E}(t) \right] \Psi(\mathbf{r},t), \tag{13}$$

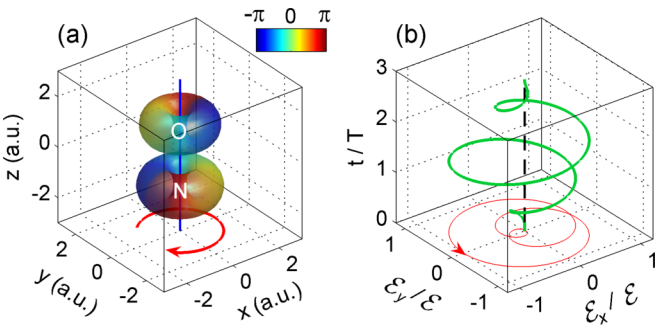

FIG. 1. (a) Current-carrying valence $2\pi_-$ orbital of NO. The contour surface of the degenerate orbital is color coded (grayscale coded) by the phase of the wave function. The vertical blue line indicates the molecular axis and the thick red arrow on the bottom the clockwise (−) electron rotation. (b) Electric field of the right (+) CP laser pulse (thick green curve) and its projection (thin red curve on the bottom) with the arrow showing the anticlockwise (+) rotation of the electric field vector.

with the effective potential of the form [16],

$$V_{\text{eff}}(\mathbf{r}) = -\sum_{k=1,2} \frac{Z_k(|\mathbf{r}-\mathbf{r}_k|)}{\sqrt{|\mathbf{r}-\mathbf{r}_k|^2 + a_k}}, \tag{14}$$

where $k = 1$ and $k = 2$ label the nuclei N and O at its fixed positions $\mathbf{r}_1 = (0,0,-R_{\text{NO}}/2)$ and $\mathbf{r}_2 = (0,0,R_{\text{NO}}/2)$ with the internuclear equilibrium distance of NO, $R_{\text{NO}} = 2.173$ a.u. The position-dependent core charge with respect to the kth nucleus $Z_k(|\mathbf{r}-\mathbf{r}_k|)$ is given by [17]

$$Z_k(r) = Z_{k,0} + Z_{k,1}e^{-r^2/\sigma_{k,1}^2} + Z_{k,2}e^{-r^2/\sigma_{k,2}^2}, \tag{15}$$

where $r = |\mathbf{r}-\mathbf{r}_k|$ is the distance from the kth nucleus to the valence electron in the 3D space. The parameters, a_k in Eq. (14) as well as $Z_{k,p}$ $(p = 0,1,2)$ and $\sigma_{k,q}$ $(q = 1,2)$ in Eq. (15), are chosen to adjust the energies of the ground $|X\,^2\Pi_\pm\rangle$ and the first excited $|A\,^2\Sigma^+\rangle$ states of NO. The values of these parameters have been adjusted and are listed in Table I. In our SAE model of NO, the numerically calculated energies of the ground and the first excited states are $E_{|X^2\Pi_\pm\rangle} = E_{2\pi_\pm} = -I_p = -0.340$ a.u. and $E_{|A^2\Sigma^+\rangle} = E_{6\sigma} = -0.132$ a.u., that coincide with corresponding experimental energies of NO. The electric field of the CP laser pulse is given by

$$\mathbf{E}_\pm(t) = \mathcal{E}\sin^2\left(\frac{\pi t}{nT}\right)[\cos(\omega t)\mathbf{e}_x \pm \sin(\omega t)\mathbf{e}_y], \tag{16}$$

where $\mathcal{E}, \omega, n$, and $T = 2\pi/\omega$ are the electric field amplitude, the laser frequency, the number of laser cycles, and the period of one laser cycle, respectively. The sign ± denotes the right (+) or left (−) circular polarization.

TABLE I. Values of the parameters used for the effective potential of NO.

	k	a_k	$Z_{k,0}$	$Z_{k,1}$	$Z_{k,2}$	$\sigma_{k,1}^2$	$\sigma_{k,2}^2$
N	1	1.7575	0.543	6.867	−0.41	2.1054	2000
O	2	1.8758	0.457	7.943	−0.40	1.8454	2000

The procedure to solve 3D TDSE numerically follows generally the method introduced in Ref. [18]. However, when applying the Crank-Nicolson method [19], we use a fourth-order (instead of second-order) central difference method for the space derivative of the discrete wave function [20], whereas we use a second-order central difference method for the time derivative. By doing this, the accuracy reaches $O((\Delta s)^4) + O((\Delta t)^2)$, which is greatly higher than the accuracy $O((\Delta s)^2) + O((\Delta t)^2)$ of the widely used second-order central differencing scheme in the Crank-Nicolson method, where Δs and Δt are space-step and time-step sizes, respectively. This improvement is important for accurate numerical calculations and useful for situations where large space-step size has to be adopted due to limited computer capabilities.

In our calculation, the time-dependent wave function is discretized on a 3D grid which ranges both for x and y from −100.7 to 100.7 a.u. and for z from −40.7 to 40.7 a.u. The grid has $1008\times1008\times408$ grid points with the same space-step size of $\Delta s = 0.2$ a.u. for all space coordinates. The time-step size for the evolution of the wave function is $\Delta t = 0.02$ a.u. The initial stationary wave functions of the $2\pi_+$ and $2\pi_-$ orbitals of NO are obtained by imaginary-time propagation and orthogonalization under symmetry conditions with respect to the azimuthal quantum number $m = \pm1$.

In the real-time propagation, we have employed the $\cos^{1/4}$-masking function to absorb the outgoing wave packet. The time-dependent ionization yield and the depletion of the initial state are calculated as $Y(t) = 1 - \langle\Psi(\mathbf{r},t)|\Psi(\mathbf{r},t)\rangle$ and $D(t) = 1 - |\langle\Psi(\mathbf{r},t)|\Psi(\mathbf{r},0)\rangle|^2$, respectively, where $\Psi(\mathbf{r},0)$ is the initial wave function, i.e., the wave function of the $2\pi_+$ or $2\pi_-$ orbital. After the pulse is off, the field-free evolution of the wave function is continued until the ionization yield and the depletion become time independent. In order to compare final ionization yields $Y_\pm$ and depletions $D_\pm$ between two initial $2\pi_\pm$ orbitals, we calculate corresponding ratios $R_Y = Y_-/Y_+$ and $R_D = D_-/D_+$ numerically.

The numerical calculations have been tested for convergence by decreasing time- and space-step sizes and increasing the grid size. Thanks to the high accuracy of the improved numerical method, the results do not change significantly for smaller time- and space-step sizes and larger grid sizes.

IV. RESULTS AND DISCUSSION

In numerical calculations of the present work, a three-cycle $(n = 3)$ right CP laser pulse is used for the ionization of the valence $2\pi_+$ and $2\pi_-$ orbitals of NO starting from the degenerate electronic ground state $|X\,^2\Pi_\pm\rangle$. These initial orbitals carry opposite stationary electron ring currents about the molecular axis. Figure 1 presents the valence $2\pi_-$ orbital of NO and the electric field of the right CP laser pulse. For the right CP laser field, the electron of the $2\pi_-$ orbital is counter-rotating with respect to the circular polarization of the laser field, as indicated by arrows on bottoms of Fig. 1, while the electron of the $2\pi_+$ orbital is co-rotating.

After solving the 3D TDSE numerically, we calculate the ratios of the ionization yields R_Y and depletions R_D between two initial $2\pi_\pm$ orbitals for six different laser wavelengths $\lambda = 400$ nm, 500 nm, 600 nm, 800 nm, 1200 nm, and 1600 nm and four different electric field amplitudes $\mathcal{E} = 0.05$ a.u.,

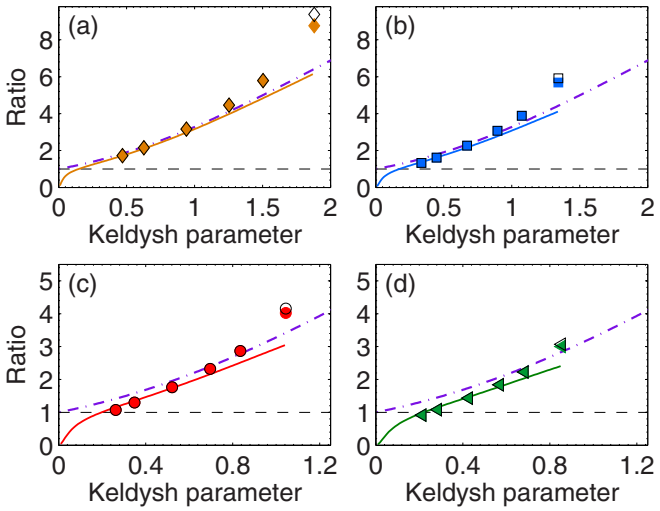

FIG. 2. Ionization ratios $R_Y = Y_-/Y_+$ (full markers) and $R_D = D_-/D_+$ (hollow markers) between two initial $2\pi_\pm$ orbitals of prealigned NO in a three-cycle right CP laser pulse, obtained from 3D-TDSE numerical calculations. The analytical ionization ratios R_+ [Eq. (8)] based on the PPT theory (dash-dotted curves) and R_+^F [Eq. (12)] including the three-level model of Floquet theory (solid curves) are also shown. The electric field amplitudes are $\mathcal{E} = 0.05$ a.u. (a), 0.07 a.u. (b), 0.09 a.u. (c), and 0.11 a.u. (d). The markers from left to right in each panel correspond to laser wavelengths $\lambda = 1600$ nm, 1200 nm, 800 nm, 600 nm, 500 nm, and 400 nm.

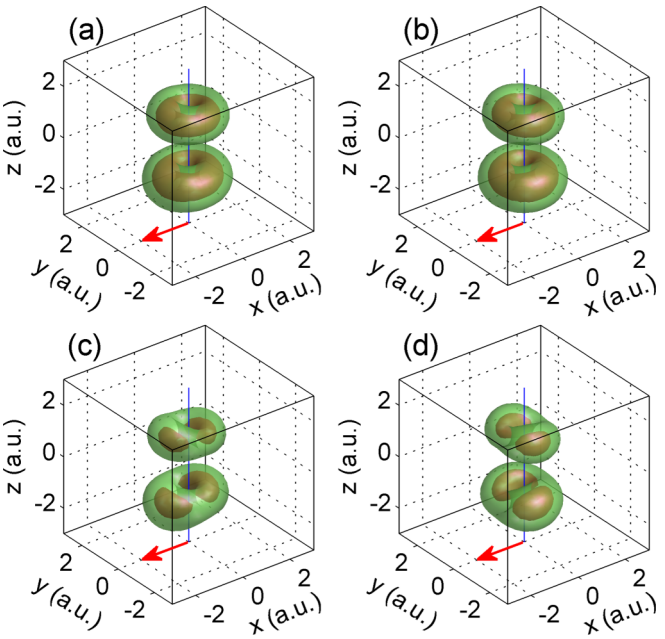

FIG. 3. Snapshots of the electron probability densities at $t = 1.5\,T$ for the initial $2\pi_+$ (left column) and $2\pi_-$ (right column) orbitals. The arrows indicate the direction of the instantaneous electric field vector. The wavelength of the three-cycle laser pulse is $\lambda = 1600$ nm and the electric field amplitudes are $\mathcal{E} = 0.05$ a.u. (top row) and 0.11 a.u. (bottom row).

0.07 a.u., 0.09 a.u., and 0.11 a.u., corresponding to laser intensities $I = 1.76\times10^{14}\,\mathrm{W/cm^2}$, $3.44\times10^{14}\,\mathrm{W/cm^2}$, $5.69\times10^{14}\,\mathrm{W/cm^2}$, and $8.50\times10^{14}\,\mathrm{W/cm^2}$. Figure 2 depicts numerical results of the ionization ratios R_Y and R_D as a function of the Keldysh parameter γ [Eq. (9)]. It shows that R_Y and R_D agree very well except for 400 nm (the rightmost markers in four panels of Fig. 2). We will show later that this deviation is due to the transient resonant excitation from the ground $|X\,^2\Pi_\pm\rangle$ state to the first excited $|A\,^2\Sigma^+\rangle$ state of NO.

For comparison, the ratios of the ionization rates for right CP laser fields R_+ [Eq. (8)] based on the PPT theory are shown as dash-dotted curves in Fig. 2. It shows that the results obtained from the PPT theory agree in general with numerical 3D-TDSE results. However, two important deviations are observed: (i) As the Keldysh parameter γ decreases, the 3D-TDSE ratios become smaller than the PPT ratios and can be even smaller than 1 [see Fig. 2(d)], indicating that the tunnel ionization of the co-rotating orbital for small γ becomes preferred. (ii) As the laser wavelength decreases, the numerically calculated 3D-TDSE ratios become larger than the PPT ratios and the deviation is most significant for $\lambda = 400$ nm. It is due to two assumptions in the PPT theory that could lead to these deviations between theory and *ab initio* calculations: (A1) The initial rotating orbital prior to tunnel ionization is assumed to be field-free bound orbital and (A2) the electronic excitation to excited states is neglected.

It has been shown that the rotating atomic $2p_\pm$ orbitals can be significantly modified by strong and low-frequency CP laser fields and become the so-called laser-dressed orbitals [8]. It leads to the change of the ionization preference of the atomic $2p_\pm$ orbitals. In order to understand whether and how the laser-dressed $\pi_\pm$ orbitals of linear molecules would affect the ionization ratio, we present in Fig. 3 four snapshots of the electron probability densities $|\Psi(\mathbf{r},t)|^2$ for both the initial valence $2\pi_\pm$ orbitals of NO and for two different 1600-nm laser pulses with $\mathcal{E} = 0.05$ a.u. and $\mathcal{E} = 0.11$ a.u. The snapshots in Fig. 3 are taken at $t = 1.5\,T$, where the electric field reaches its maximum and the instantaneous electric field vector is directed in the negative x direction. For the laser pulse with low intensity, there is no obvious modification of the $2\pi_\pm$ orbitals by laser fields. Thus, the PPT theory still works well within the assumption (A1). However, for the laser pulse with high intensity, we can see that the $2\pi_\pm$ orbitals are strongly modified by laser fields. The $2\pi_+$ orbital is adiabatically modified to the laser-dressed $2\pi_\parallel$ orbital and it is aligned along the electric field vector [Fig. 3(c)], making the electron tunnel more easily. In contrast, the $2\pi_-$ orbital is adiabatically modified to the laser-dressed $2\pi_\perp$ orbital and it is aligned perpendicularly to the electric field vector [Fig. 3(d)], leading to the ionization suppression of the $2\pi_-$ orbital. The ratios of the ionization yields R_Y and depletions R_D are therefore reduced for strong and low-frequency CP laser fields, not only for atoms [8] but also for linear molecules.

To account for the ionization ratio of laser-dressed orbitals, we have improved our theory by including the three-level model of Floquet theory, i.e., by setting the Floquet wave function [Eq. (11)] as the initial wave function prior to tunnel ionization in the derivation of the formulas of the ionization rates in the PPT theory. The improved analytical result for the ionization ratio for atomic or molecular orbitals with $m = \pm1$ is given in Eq. (12). For $2\pi_\pm$ orbitals of NO, this improved

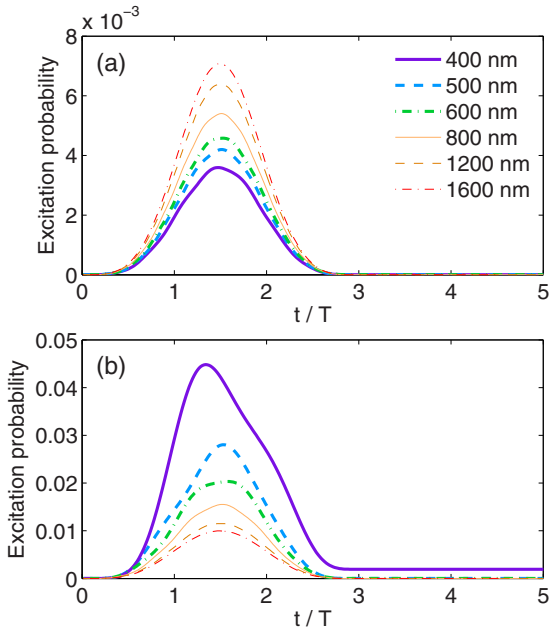

FIG. 4. Transient excitation probabilities from the valence $2\pi_+$ (a) or $2\pi_-$ (b) orbital to the first excited 6σ orbital of NO for different laser wavelengths. The field amplitude is $\mathcal{E} = 0.07$ a.u.

result (PPT+Floquet theory) is presented as solid curves in Fig. 2. Comparing this improved result with the original result (PPT without Floquet theory) presented as dash-dotted curves in Fig. 2 clearly shows that after considering the Floquet theory for laser-dressed orbitals, the numerical 3D-TDSE results are very well predicted by our improved theory (PPT+Floquet theory) for small γ.

Next, we will discuss the deviation of the ionization ratios for short laser wavelengths. One obvious tendency shown in Fig. 2 is that, as the laser frequency increases, the numerically calculated ratios become significantly larger than the theoretical ratios. Though the similar phenomenon was also observed for atomic $2p_\pm$ orbitals [8], the underlying mechanism was not clear yet. Here, we will show that such deviation is due to the assumption (A2) of the PPT theory. In Fig. 4, we present the transient excitation probabilities $|\langle\Psi(\mathbf{r},\mathbf{t})|\Psi_{6\sigma}(\mathbf{r})\rangle|^2$ from the valence $2\pi_\pm$ orbital to the first excited 6σ orbital $\Psi_{6\sigma}(\mathbf{r})$ during the interaction of NO with the right CP laser pulse for different laser wavelengths. It corresponds to the excitation from the ground $|X\,^2\Pi_\pm\rangle$ state to the first excited $|A\,^2\Sigma^+\rangle$ state in the SAE approximation. It shows that the magnitude of the excitation probability for the $2\pi_+$ orbital decreases with decreasing the laser wavelength, while the tendency is just opposite for the $2\pi_-$ orbital. Note that the same wavelength-dependent excitation tendencies for other laser intensities are also observed in our numerical calculations. Since the electronic excitation enhances the ionization yield (due to lower ionization potentials of excited states), the opposite dependencies of the transient excitation on the laser wavelength shown in Fig. 4 indicate that for short laser wavelengths the electron of the $2\pi_-$ orbital after transient excitation is more easily removed than that of the $2\pi_+$ orbital. Therefore, the effect of the transient excitation on subsequent ionization, that is unfortunately not considered in the PPT theory, further enhances the ionization ratio between $2\pi_\pm$ orbitals, leading to the deviation between numerical 3D TDSE and theoretical PPT results for short laser wavelengths.

Furthermore, Fig. 4(b) shows the anomalous transient excitation of the 6σ orbital for the interaction of the $2\pi_-$ orbital with the 400 nm right CP laser pulse. The corresponding transient excitation probability is significantly larger than others. This enhancement could arise from the resonant excitation from the $2\pi_-$ orbital to the excited 6σ orbital of NO. Although the corresponding orbital energies are separated by about 220 nm and maybe modified by Stark effect, the broad bandwidth of the few-cycle strong laser pulse could make this resonant excitation possible; cf. Ref. [21]. After the laser pulse is off, a part of the wave function for the initial $2\pi_-$ orbital and for 400-nm laser pulses remains in the excited orbital 6σ, that leads to the obvious deviation between the numerical ratios of the ionization yields and depletions between initial $2\pi_\pm$ orbitals, as shown in Fig. 2.

So far, we have shown that the ionization in CP laser fields is sensitive to the sense of electron rotation not only for atoms but also for prealigned linear molecules. Such sensitivity indeed offers the opportunity to produce highly spin-polarized photoelectrons and ions; cf. Ref. [9]. In the presence of spin-orbit coupling, the electronic ground state $|X\,^2\Pi_\pm\rangle$ of the NO molecule is split into two doubly degenerate states, the energetically lowest $|X\,^2\Pi_{1/2}\rangle$ and excited $|X\,^2\Pi_{3/2}\rangle$ states, separated by about $120\,\mathrm{cm}^{-1}$ (0.015 eV). The $|X\,^2\Pi_{1/2}\rangle$ state has two possible valence electron configurations $2\pi_-^\uparrow$ ($m_j = -1/2$) and $2\pi_+^\downarrow$ ($m_j = 1/2$), whereas the $|X\,^2\Pi_{3/2}\rangle$ state has two other possible valence electron configurations $2\pi_-^\downarrow$ ($m_j = -3/2$) and $2\pi_+^\uparrow$ ($m_j = 3/2$). According to results shown in Fig. 2, the electron from the $2\pi_-$ orbital tunnels more easily for moderately strong right CP laser fields. Starting from the electronic ground state $|X\,^2\Pi_{1/2}\rangle$, the electron from the valence $2\pi_-^\uparrow$ spin orbital is therefore more easily removed than that from the $2\pi_+^\downarrow$ spin orbital. It results in the generation of the large amount of spin-up photoelectrons. Similarly, starting from the $|X\,^2\Pi_{3/2}\rangle$ state, the electron from the valence $2\pi_-^\downarrow$ spin orbital is more easily removed and it yields the large amount of spin-down photoelectrons. Compared to the spin polarization up to 50% produced from fourfold degenerate lowest ionic states $|X\,^2P_{3/2}\rangle$ of noble gas atoms [9], lower degeneracy in linear molecules can cause effective control of spin polarization of photoelectrons and molecular ions up to 100%. Figures 5(a) and 5(b) depict the spin polarizations of the photoelectrons as a function of Keldysh parameter γ for the initial $|X\,^2\Pi_{1/2}\rangle$ and $|X\,^2\Pi_{3/2}\rangle$ states driven by right CP laser pulses, calculated as

$$\mathcal{P}_{1/2} = -\frac{1-R}{1+R}, \tag{17}$$

$$\mathcal{P}_{3/2} = +\frac{1-R}{1+R}, \tag{18}$$

where R is the ionization ratio (R_+, R_+^F, R_Y, R_D), respectively. The numerical results agree well with theoretical results. It shows that the spin polarization can be manipulated by varying the laser frequency and the laser intensity. In principle, up to

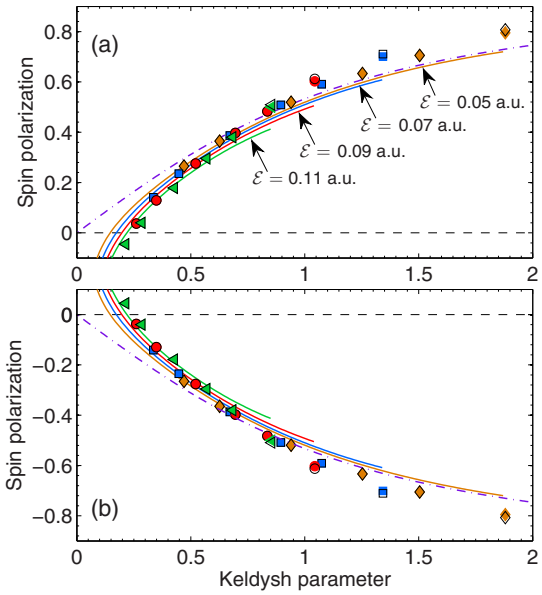

FIG. 5. Spin polarization of the photoelectron induced by strong-field tunnel ionization of the electronic $|X\,^2\Pi_{1/2}\rangle$ (a) and $|X\,^2\Pi_{3/2}\rangle$ (b) states of NO. The positive and negative values of the spin polarization indicate dominant amounts of spin-up and spin-down photoelectrons, respectively. The different curves and markers are the same as used in Fig. 2.

100% spin polarization can be achieved in the experiment via energy separation of the electronic $|X\,^2\Pi_{1/2}\rangle$ and $|X\,^2\Pi_{3/2}\rangle$ states of NO.

Without considering the spin-orbit splitting, the degenerate ground $|X\,^2\Pi_{\pm}\rangle$ state of NO consists of 50%$|X\,^2\Pi_{+}\rangle$ state ($2\pi_+$ orbital) and 50% $|X\,^2\Pi_{-}\rangle$ state ($2\pi_-$ orbital). To investigate the dependence of the tunnel ionization of NO on the initial current-carrying $2\pi_+$ and $2\pi_-$ orbitals in the experiment, we propose one possible scheme to select the $2\pi_+$ or $2\pi_-$ orbital of prealigned NO. Here, we focus on the detail for the selection of the $2\pi_+$ orbital, i.e., the selection of the $|X\,^2\Pi_{+}\rangle$ state. A relatively weak and long right CP laser pulse with the photon energy equal to the energy gap between the ground $|X\,^2\Pi_{\pm}\rangle$ and the first excited $|A\,^2\Sigma^{+}\rangle$ states propagates along the axis of the NO molecule. By electric dipole transition, the $2\pi_-$ orbital is resonantly excited to the excited 6σ orbital by absorbing one photon. This 6σ orbital is subsequently ionized by absorbing a second photon. In contrast, due to the weakness of the electric field and the selection rules for electric dipole transitions, the other $2\pi_+$ orbital cannot be excited and ionized. It indicates that the degenerate $|X\,^2\Pi_{+}\rangle$ (or $|X\,^2\Pi_{-}\rangle$) state can be selected and the initial direction of the electron rotation of the selected $2\pi_+$ (or $2\pi_-$) orbital is known.

V. CONCLUSIONS AND OUTLOOK

In the present paper, we have derived the analytical formula of the ionization ratio between degenerate valence molecular $\pi_\pm$ orbitals of prealigned linear molecules in strong CP laser fields. It was derived based on the PPT theory and then improved by using the three-level model of Floquet theory to account for the correct description of the nonadiabatic tunnel ionization of laser-dressed orbitals in strong and low-frequency laser fields. In particular, we have shown that the analytical expressions for the ionization ratio for atomic and molecular orbitals with opposite magnetic (azimuthal) quantum numbers $m = \pm 1$ are equal, i.e., the ratio of the ionization rates of atomic $p_\pm$ and molecular $\pi_\pm$ orbitals depending on Keldysh parameter γ are equal.

We have also verified our theoretical predication by performing numerical 3D-TDSE calculations within the SAE approximation for ionization of the valence molecular $2\pi_\pm$ orbitals of the prealigned NO molecule. In fact, the numerical results agree very well with theoretical PPT results. Two observed deviations between these results for relatively strong and low-frequency laser fields and for high-frequency laser fields were also discussed in this paper. In particular, for strong and low-frequency laser fields, the deviation is due to adiabatically modified (laser-dressed) orbitals prior to tunnel ionization that can cause the change of the ionization preference of degenerate atomic and molecular orbitals. Using PPT+Floquet theory, the numerical results for strong and low-frequency laser fields agree well with theoretical results for ionization of laser-dressed orbitals. For high-frequency laser fields, we have analyzed the excitation probabilities of the excited 6σ orbital of NO and shown that the deviation between numerical and theoretical results comes from the transient resonant excitation from $2\pi_-$ (in case of right circular polarization) to 6σ orbitals and subsequent ionization of the 6σ orbital.

Finally, due to spin-orbit coupling of the electronic ground state $|X\,^2\Pi_{\pm}\rangle$ of NO, that splits into two doubly degenerate $|X\,^2\Pi_{1/2}\rangle$ and $|X\,^2\Pi_{3/2}\rangle$ states, and due to ionization preference of the counter-rotating orbital with respect to the circular polarization of the laser field, highly spin-polarized (up to 100%) photoelectrons can be produced by nonadiabatic tunnel ionization of the $|X\,^2\Pi_{1/2}\rangle$ or $|X\,^2\Pi_{3/2}\rangle$ state. Furthermore, the spin polarization depends sensitively on the electric field amplitude and the frequency of the CP laser field.

In the near future, we will analyze 3D photoelectron momentum distributions (PMD) for electrons removed from valence $2\pi_\pm$ orbitals of NO in strong CP laser pulses. We expect that the angular shifts in PMDs are different for oppositely current-carrying molecular $\pi_\pm$ orbitals (see Ref. [22] for atomic $p_\pm$ orbitals) and the direction of the initial electronic ring currents of the molecular $\pi_\pm$ orbitals could be detected in attoclock experiments; cf. Refs. [23,24]. Note that the strong-field tunnel ionization imaging of photoexcitation of NO has been already demonstrated in the experiment [25]. In addition, we will also analyze momentum- and angle-resolved spin polarization of photoelectrons from NO. Very recently, spin-polarized photoelectrons produced by tunnel ionization of noble gas in strong bichromatic or monochromatic CP laser pulses have been found in the theory and in the experiment (see Refs. [26] and [27]), respectively. We also expect nonzero spin polarization of photoelectrons from degenerate orbitals of nonaligned linear molecules. The effect of nonalignment on spin polarization will be analyzed in detail soon. Finally, our next goal is to investigate nonadiabatic tunnel ionization of degenerate $e_\pm$ orbitals of ring-shaped molecules (for example, benzene) in strong CP laser fields.

ACKNOWLEDGMENTS

This work was financially supported by the Max Planck Society for the Max Planck Research Group "Current-Carrying Quantum Dynamics" (CCQD) and by the Deutsche Forschungsgemeinschaft, Priority Programme 1840 "Quantum Dynamics in Tailored Laser Fields" (QUTIF).

[1] A. M. Perelomov, V. S. Popov, and M. V. Terent'ev, Sov. Phys. JETP **23**, 924 (1966).
[2] A. M. Perelomov, V. S. Popov, and M. V. Terent'ev, Sov. Phys. JETP **24**, 207 (1967).
[3] A. M. Perelomov and V. S. Popov, Sov. Phys. JETP **25**, 336 (1967).
[4] I. Barth and O. Smirnova, Phys. Rev. A **84**, 063415 (2011); **85**, 029906(E) (2012); **85**, 039903(E) (2012).
[5] I. Barth and O. Smirnova, Phys. Rev. A **87**, 013433 (2013).
[6] T. Herath, L. Yan, S. K. Lee, and W. Li, Phys. Rev. Lett. **109**, 043004 (2012).
[7] I. Barth and O. Smirnova, Phys. Rev. A **87**, 065401 (2013).
[8] I. Barth and M. Lein, J. Phys. B **47**, 204016 (2014).
[9] I. Barth and O. Smirnova, Phys. Rev. A **88**, 013401 (2013).
[10] I. Barth, J. Manz, and L. Serrano-Andrés, Chem. Phys. **347**, 263 (2008).
[11] I. Barth, L. Serrano-Andrés, and T. Seideman, J. Chem. Phys. **129**, 164303 (2008).
[12] X. M. Tong, Z. X. Zhao, and C. D. Lin, Phys. Rev. A **66**, 033402 (2002).
[13] S.-F. Zhao, C. Jin, A.-T. Le, T. F. Jiang, and C. D. Lin, Phys. Rev. A **81**, 033423 (2010).
[14] S. V. Popruzhenko, V. D. Mur, V. S. Popov, and D. Bauer, Phys. Rev. Lett. **101**, 193003 (2008).
[15] J. Kaushal and O. Smirnova, Phys. Rev. A **88**, 013421 (2013).
[16] M. Peters, T. T. Nguyen-Dang, E. Charron, A. Keller, and O. Atabek, Phys. Rev. A **85**, 053417 (2012).
[17] X. M. Tong and C. D. Lin, J. Phys. B **38**, 2593 (2005).
[18] N. Watanabe and M. Tsukada, Phys. Rev. E **62**, 2914 (2000).
[19] J. Crank and P. Nicolson, Adv. Comput. Math. **6**, 207 (1996).
[20] B. Fornberg, Math. Comp. **51**, 699 (1988).
[21] X. Zhu, P. Lan, K. Liu, Y. Li, X. Liu, Q. Zhang, I. Barth, and P. Lu, Opt. Express **24**, 4196 (2016).
[22] J. Kaushal, F. Morales, and O. Smirnova, Phys. Rev. A **92**, 063405 (2015).
[23] P. Eckle, M. Smolarski, P. Schlup, J. Biegert, A. Staudte, M. Schöffler, H. G. Muller, R. Dörner, and U. Keller, Nat. Phys. **4**, 565 (2008).
[24] A. N. Pfeiffer, C. Cirelli, M. Smolarski, D. Dimitrovski, M. Abu-samha, L. B. Madsen, and U. Keller, Nat. Phys. **8**, 76 (2012).
[25] T. Endo, A. Matsuda, M. Fushitani, T. Yasuike, O. I. Tolstikhin, T. Morishita, and A. Hishikawa, Phys. Rev. Lett. **116**, 163002 (2016).
[26] D. B. Milošević, Phys. Rev. A **93**, 051402(R) (2016).
[27] A. Hartung, F. Morales, M. Kunitski, K. Henrichs, A. Laucke, M. Richter, T. Jahnke, A. Kalinin, M. Schöffler, L. P. H. Schmidt, M. Ivanov, O. Smirnova, and R. Dörner, Nat. Photon. **10**, 526 (2016).